Prospects of Squark & Slepton searches at a Gamma Gamma Collider

Debajyoti Choudhury[1] and Anindya Datta[2]

Mehta Research Institute, Chhatnag Road, Jhusi, Allahabad 211 019, India.

E-mail: [1]debchou@.mri.ernet.in, [2]anindya@mri.ernet.in

Abstract

We examine the prospects of detecting sfermions at a gamma gamma collider. Once produced, a slepton can decay into a pair of quarks (jets) through R-parity violating interactions. Similarly, a squark may decay into a lepton-quark pair. Analyzing the corresponding Standard Model backgrounds, namely 4-jet and dilepton plus dijet final states respectively, we show that the sfermion can be detected almost right upto the kinematic limit and its mass determined to a fair degree of accuracy. Similar statements also hold for nonsupersymmetric leptoquarks and diquarks.

PACS numbers: 12.60.Jv, 14.80.Ly, 13.88.+e

1 Introduction

The Standard Model (SM) of electroweak interactions, while eminently successful in describing most available data, is rightly not regarded as the final theory. Apart from aesthetic drawbacks such as the lack of explanations for either the fermion masses or the relative strength of the gauge couplings, it also suffers from a few technical problems. To overcome these lacunae, many authors have, over the years, proposed models going beyond the SM. Two of the most attractive classes of such models are those incorporating grand unification [1] and/or supersymmetry [2]. Both, as well as other models, predict additional particle states. In this article we shall concentrate on the scalar sector of such theories.

Within the SM, baryon (B) and lepton (L) number conservation come about due to accidental symmetries. In other words, such conservation is not guaranteed by any theoretical reasons, but are rather the consequences of the choice of the particle content[1]. In extensions of the SM, such an accidental occurrence is obviously not guaranteed. For example, even in the simplest grand unified theories (GUTs), both

---

[1]Indeed, nonperturbative effects within the SM itself do break $B + L$ symmetry.

the gauge and the scalar sector interactions violate each of B and L. The corresponding particles, namely the diquarks [3] and leptoquarks [4] have been studied in the literature to a considerable extent. Simultaneous breaking of both B and L symmetry can be disastrous though as that would lead to rapid proton decay. Within GUTs, gauge boson-mediated proton decay is naturally suppressed on account of their large mass; in the scalar sector, the particle content can be chosen such that there is no diquark-leptoquark mixing, at least as far as the light sector is concerned.

In the case of the Minimal Supersymmetric Standard Model (MSSM), on the other hand, we do not have the option of demanding the 'offending' fields (the supersymmetric partners of the SM fermions) to be superheavy. Ruling out the undesirable terms necessitates the introduction of a discrete symmetry, $R \equiv (-1)^{3(B-L)+2S}$ (with S denoting the spin of the field) [5]. Apart from ruling out both B and L violating terms in the superpotential, this symmetry has the additional consequence of rendering the lightest supersymmetric partner absolutely stable. However, such a symmetry is *ad hoc*. Hence, it is of interest to consider possible violations of this symmetry especially since it has rather important experimental consequences, not the least of which concerns the detection of the supersymmetric partners.

As we shall see later, there are certain similarities between $\not{R}$ interactions on the one hand and leptoquarks and/or diquarks on the other. An example of this is afforded by the explanations [6] of the anomalous large-Q^2 data reported by the HERA collaborations. However, the $\not{R}$-MSSM, being a richer (low-energy) theory, offers a larger set of possibilities, both in the context of the HERA events as well as other anomalies like the ones observed at KARMEN[7] or at KAMIOKANDE[8]. Hence, in our discussions, we shall concentrate primarily on the supersymmetric case, and point out, as special cases, the corresponding results for theories with leptoquarks or diquarks.

It is only natural that such particles would be looked for in existing colliders. Indeed, the best lower bounds on the masses of such particles have been obtained from analyses Tevatron data. Pair production of leptoquarks (or equivalently squarks decaying through an L violating interaction) leads to a final state comprising a dilepton pair alongwith jets [9]. More interestingly, in the supersymmetric case, gluino production cross-section is larger and, in addition, can lead to like-sign dileptons, thereby making the signal stand out even more [10]. However, all such analyses, of necessity, make certain assumptions that are not necessarily true. Similar is the case of searches at HERA which depend on the size of the L-violating coupling [11]. To minimize the dependence on such assumptions, it is thus necessary to consider further experiments.

In this article we investigate the production of such scalars (supersymmetric or otherwise) at a photon collider. The lepton (or baryon) number violating decays may result in a significant excess in dijet plus dilepton or 4-jet final states. An analysis of such data would allow us not only to detect such particles but also to measure their masses and, to an extent, the branching fractions. The plan of the rest of the article is as follows. In the next section we discuss briefly the photon photon collider and the production cross-section of these scalar fermions at a such a collider. In section 3, we focus on the $\not{R}$ violating couplings and the decays of the squarks and the sleptons. Section 4 will be devoted to comparing the signals and the possible SM backgrounds.

We will explore the discovery/ exclusion limits on the SUSY parameter space using our signal and background analysis in section 5. Finally, we summarise in section 6.

2   Pair-production of Scalars at a Photon Collider

To the leading order in perturbation theory, the cross-section for charged particle pair-production at a gamma gamma collider is completely model independent This is quite unlike the case for the e^+e^- machine where the coupling of the scalar to the Z as well as its Yukawa couplings have a bearing on the answer. Thus, model dependence appears only in the decay channels, and hence is easier to analyse. Let us consider, first, the case of monochromatic photon beams. If the center-of-mass energy be $\sqrt{s}$, and the product of the photon helicities (circular polarization)^2 be $P_{\gamma\gamma}$, the pair-production cross-section for a scalar of charge Q and mass m is given by

$$\frac{\mathrm{d}\sigma}{\mathrm{d}\Omega} = \frac{Q^4 N_c \alpha^2}{s} \beta \left[(1 + P_{\gamma\gamma}) \left\{ \frac{1}{2} - \frac{\beta^2 \sin^2 \theta}{1 - \beta^2 \cos^2 \theta} \right\} + \frac{\beta^4 \sin^4 \theta}{(1 - \beta^2 \cos^2 \theta)^2} \right]. \qquad (1)$$

In eq.(1), $\beta \equiv (1 - 4m^2/\hat{s})$ is the velocity of the scalars in the center of mass frame and θ the corresponding scattering angle. The colour factor $N_c = 1(3)$ for sleptons (squarks). The unpolarised cross-section can easily be obtained from the above expression by setting $P_{\gamma\gamma} = 0$. One can check easily that, for small scalar masses, the dominant mode is the $P_{\gamma\gamma} = -1$ mode. On the other hand, the $P_{\gamma\gamma} = 1$ mode dominates for scalar masses near the kinematic limit [13].

In reality though, high energy monochromatic photon beams are extremely unlikely. In fact, the only known way to obtain very high energy photon beams is to induce laser back-scattering off an energetic $e^\pm$ beam [14]. The reflected photon beam carries off only a fraction (y) of the $e^\pm$ energy with

$$\begin{aligned} y_{\max} &= \frac{z}{1+z} \\ z &\equiv \frac{4 E_e E_L}{m_e^2} \cos^2 \frac{\theta_{eL}}{2} \end{aligned} \qquad (2)$$

where $E_{e(L)}$ are the energies of the incident $e^\pm$ beam and the laser respectively and θ_{eL} is the incidence angle. One can, in principle, increase the photon energy by increasing the energy of the laser beam. However, increasing E_L also enhances the probability of electron positron pair creation through laser and scattered-photon interactions, and consequently results in beam degradation. An optimal choice of z taking care of this is $z = 2(1 + \sqrt{2})$, and this is the value that we adopt in our analysis.

The cross-sections for a realistic photon-photon collider can then be obtained by convoluting the fixed-energy cross-sections of eq.(1) with the appropriate photon spectrum. For circularly polarized lasers scattering off polarised electron beams, the

---

^{2}We do not consider here the possibility of linear polarization. The most general expression can be found in Ref. [13].

number-density $n(y)$ and average helicity $\xi(y)$ for the scattered photons are given by [14]

$$
\begin{aligned}
\frac{dn}{dy} &= \frac{2\pi\alpha^2}{m_e^2 z \sigma_C} C(y) \\
\xi(y) &= \frac{1}{C(y)}\left[P_e\left\{\frac{y}{1-y} + y(2r-1)^2\right\} - P_l(2r-1)\left(1-y+\frac{1}{1-y}\right)\right] \quad (3) \\
C(y) &\equiv \frac{y}{1-y} + (1-y) - 4r(1-r) - 2P_e P_l r z(2r-1)(2-y)
\end{aligned}
$$

where $r \equiv y/z/(1-y)$ and σ_C is the total Compton cross-section. In the study of polarized beams, one fact needs to be borne in mind. While full (100%) polarisation is possible for a laser, it is unlikely to be realized for electrons. In the rest of this article we shall consider the electron polarization, wherever applicable, to be 90%.

In Fig.1, we present the total cross-section for slepton pair production at a photon collider wherein the parent e^+e^- (or e^-e^-) collider operates at a center of mass energy of 1 TeV. We present the results for three combinations of incident laser and electron polarizations ($L_1 e_1 L_2 e_2$). For the entire mass range, at least one of the two polarised ($+ + ++$ and $+ - +-$) cross-sections wins over the unpolarised case. When scalar masses are less than 230 GeV, cross-section for all three cases are comparable with $\sigma_{++++} > \sigma_{\rm unp} > \sigma_{+-+-}$. But for scalar masses above 230 GeV this hierarchy is just the opposite. In this region, σ_{+-+-} falls off more slowly than the other two. Depending on $m_{\tilde{f}}$, σ_{+-+-} can be 5–8 times larger than $\sigma_{\rm unp}$ in this mass range.
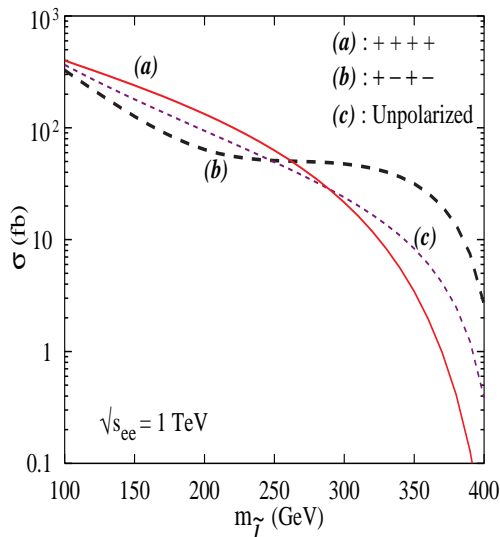

Figure 1: *Cross-section for slepton production at a $\gamma\gamma$ collider*

3   R-parity Violating Decays of the Sfermions.

In this section we present a very brief overview of the phenomenology of R-parity violation within the MSSM with particular emphasis on the additional decay channels

available to the sfermions. As has been noted in the literature, unless a discrete symmetry is introduced explicitly, the superpotential, in addition to the normal Yukawa terms, can also contain the following terms:

$$\mathcal{W}_{\not{R}} = \mu_i L_i H_2 + \lambda_{ijk} L_L^i L_L^j \bar{E}_R^k + \lambda'_{ijk} L_L^i Q_L^j \bar{D}_R^k. + \lambda''_{ijk} \bar{U}_R^i \bar{D}_R^j \bar{D}_R^k. \tag{4}$$

In the above, while L_L^i and Q_L^i denote the left-handed lepton and quark doublet superfields respectively, E_R^i, U_R^i and D_R^i denote the corresponding right-handed superfields. The couplings λ_{ijk} are antisymmetric under the exchange of the first two indices, while λ''_{ijk} are antisymmetric under the exchange of the last two. Since the 36 couplings λ_{ijk} and λ'_{ijk} violate lepton-number while the other 9 (λ''_{ijk}) violate baryon number, simultaneous existence of both the sets of operators would lead to a rapid proton decay and is hence strongly disfavoured. We will thus consider either L violating or B violating couplings. Furthermore, even within one such subset, non-zero values of more than one coupling could lead to large flavour-changing neutral current amplitudes [12]. We will thus restrict ourselves to cases where only one such coupling is dominant[3].

Examining the individual couplings *vis a vis* direct $\not{R}$ decays of sfermions, we easily notice:

- the couplings λ_{ijk} connect either a charged slepton to a lepton-neutrino pair or a sneutrino to two charged leptons. While sneutrino pair production is irrelevant in the context of photon colliders, charged sleptons will lead to a final state with a lepton pair and missing energy-momentum, a state with a large SM background emanating from W-pair production;

- the couplings λ'_{ijk} lead to both squark-quark-lepton and slepton-quark-quark vertices. While the first resembles a leptoquark vertex, the second (apart from colour factors) mimics a diquark vertex (although there is no violation of baryon number);

- the couplings λ''_{ijk} lead to squark-quark-quark vertices, and again mimic diquarks as far as direct $\not{R}$ decays are concerned.

Thus direct decays through λ_{ijk} are of no concern to us. Since we shall not address the question of cascading decays in this article, we do not consider such couplings any further. Similarly, as far as direct decays are concerned, the phenomenology of λ''_{ijk} is very similar to that of slepton pair production and subsequent decay through some λ'_{ijk}. Hence it suffices to consider the case of a single non-zero λ'_{ijk}. Analogous results for λ''_{ijk} can easily be deduced from those that we present.

Expressed in terms of the component fields, the relevant part of the Lagrangian reads

$$
\begin{aligned}
\mathcal{L}_{\lambda'} \;=\; \lambda'_{ijk} \Big[& \tilde{\nu}_L^i \bar{d}_R^k d_L^j + \tilde{d}_L^j \bar{d}_R^k \nu_L^i + (\tilde{d}_R^k)^* (\bar{\nu}_L^i)^c d_L^j \\
& - \tilde{e}_L^i \bar{d}_R^k u_L^j - \tilde{u}_L^j \bar{d}_R^k e_L^i - (\tilde{d}_R^k)^* (\bar{e}_L^i)^c u_L^j \Big] + h.c
\end{aligned}
\tag{5}
$$

---

[3]This assumption, of course, prevents us from considering certain spectacular collider signatures.

Bounds on these couplings can be obtained from various low-energy observables [15]. These include, for example, meson decay widths [16], neutrino masses [17], rates for neutrinoless double beta decay [18] *etc.* The bounds generally scale with the sfermion mass, and for $m_{\tilde{f}} = 100$ GeV range from ~ 0.02 to 0.8.
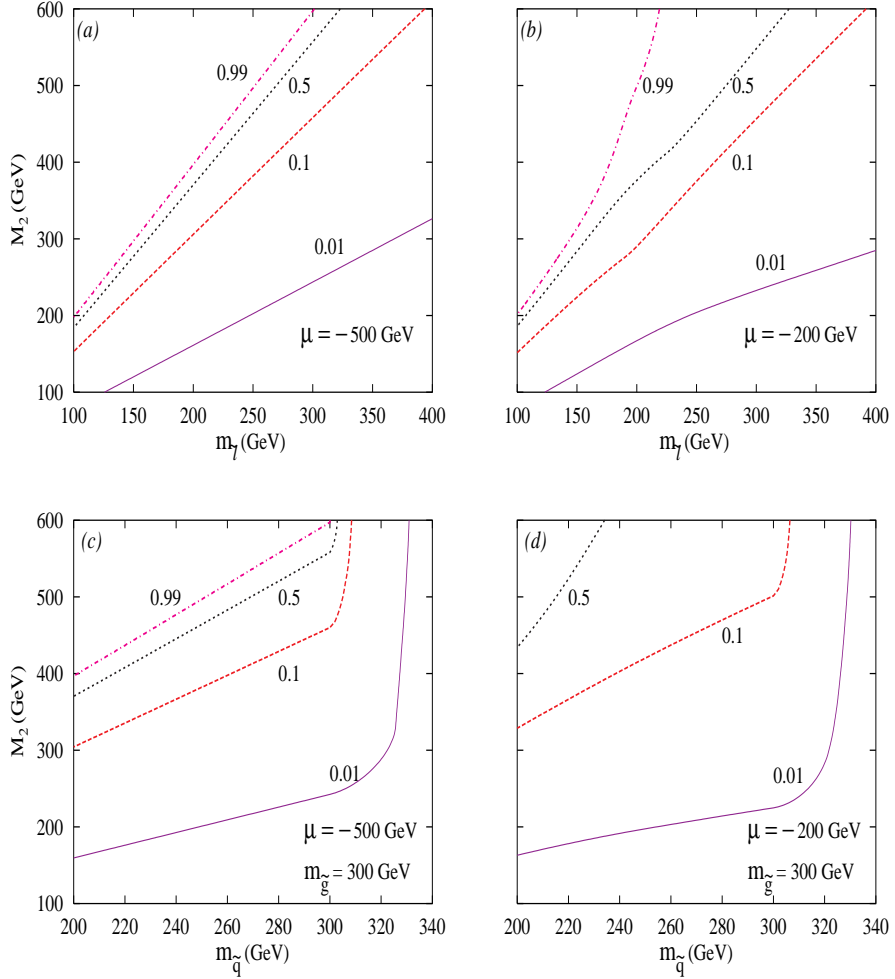

Figure 2: *Contours for constant $\not{R}$- decay branching ratios. (a) slepton with $\mu = -500$ GeV, (b) slepton with $\mu = -200$ GeV, (c) squark with $\mu = -500$ GeV and (d) squark with $\mu = -200$ GeV. In each case, $\lambda' = 0.02$, $\tan\beta = 5$. For squark decays, we have assumed the gluino mass to be 300 GeV.*

In presence of such a $\not{R}$ term, a sfermion can decay into two SM fermions. This mode then competes with the R-conserving ones namely $\tilde{f} \to f + \chi_i^0$, $f' + \chi_i^{\pm}$. The partial decay widths for the latter are of course determined by the masses of the neutralinos (charginos) and their couplings to the sfermion. These quantities, in turn, are determined by the gaugino mass parameters M_i, the higgsino mass μ and the ratio of the two higgs vacuum expectation values $\tan\beta$. However, if decays into the top quark are not allowed, the dependence on the last two parameters is negligible. Furthermore, if we assume gaugino mass unification, as happens in GUTs or supergravity inspired scenarios, only one of the parameters M_i is independent. In Fig.2, we

plot the contours of constant $\not{R}$-branching ratios for sleptons and up-type squarks in M_2-$m_{\tilde{f}}$ plane. The particular value of λ'_{ijk} chosen here satisfies the strongest (barring the case of λ'_{111}) of the low energy constraints for $m_{\tilde{f}} \gtrsim 100$ GeV. To reduce the number of parameters, we assume the GUT relation between the $U(1)$ and $SU(2)$ gaugino masses but retain the gluino mass as a free parameter. The lower limit on the squark mass has been chosen so as to be consistent[4] with the bounds quoted by the CDF collaboration [9].

Let us concentrate first on Fig.2a, where we consider the case of a slepton and $\mu = -500$ GeV. The higgsino mass being large, two of the neutralinos (as well as one chargino state) are irrelevant over the entire range of parameter space displayed. The slepton may only decay into the two lighter neutralinos (mainly gauginos) and the lighter chargino. The straight lines thus reflect contours of equal kinematic suppression in the decay widths. The curves change somewhat for a smaller value of μ (see Fig.2b) since now the neutralino (chargino) sector mixings ensure that more decay channels are available to the slepton (especially if it is on the heavier side).

For smaller masses, the contours for the squarks (Figs.2c, d) are qualitatively similar. The main difference arises on account of the gluino, which we assume, for the purpose of the graph, to be significantly lighter than that stipulated by gaugino mass unification. Since the decay into gluino proceeds through strong interactions, it dominates almost immediately on crossing the kinematic threshold. It must be pointed out though that, for the stop, this decay (or, for that matter, the decays into neutralinos) almost never reaches the kinematic threshold in the parameter range of interest.

4 Signals and Backgrounds

We are now in a position to discuss the signals that we are interested in and the backgrounds thereof. As already discussed, we focus on the direct $\not{R}$–decays of the sfermions. Thus, the sleptons decay into two quarks each, while for the squarks we concentrate on $l(e, \mu) + jet$. Thus, the pair produced charged scalars will give rise to l^+l^- plus 2 jet or 4 jet in the final state.

The obvious background consists of the SM process $\gamma\gamma \rightarrow 4$ fermions. This has contributions from both 'resonant' (such as W^+W^- production) and nonresonant diagrams. Another potential source is heavy quark (b, c) production followed by decays of these quarks. However, in general such decay products are soft and such backgrounds can be eliminated by imposing simple kinematical cuts. Also to be considered are the contributions from both single– and double–resolved processes. These turn out to be negligible though. The large number of diagrams contributing to the background are calculated using the helicity amplitude package MADGRAPH [19]. To estimate the number of events and their distribution(s), we use a parton-level Monte-Carlo event generator.

---

[4]In actuality, their bound is somewhat larger than 200 GeV, but has been obtained for a special case.

4.1 Squark Production

We begin with the squarks as the analysis is simpler. To be specific, we consider only the up-type $(Q = 2/3)$ squarks as the production cross-section is 16 times than that for the down-type squarks. The only direct $\not{R}$ decay channel is therefore into a charged lepton and a down-type quark with the resultant final state consisting of two hard jets alongwith two hard leptons.

For given quark and lepton flavours, there are *forty* SM diagrams contributing to the the process $\gamma\gamma \to \ell^+\ell^- q\bar{q}$. These can be divided into three topological classes:

- 12 of the type $\gamma\gamma \to \ell^+\ell^-\gamma^*(Z^*)$ with the off-shell boson emanating from any of the three lepton lines and subsequently going into the quark pair;

- 12 of the type $\gamma\gamma \to q\bar{q}\gamma^*(Z^*)$;

- 16 diagrams with a 't-channel' $\gamma(Z)$ exchange (nonresonant topology).

Clearly, for small angle scatterings, each of these diagrams can lead to a large contribution. To eliminate these, we require that both jets and leptons should be relatively central:

$$|\eta_{j,\ell}| < 2.5 . \tag{6}$$

This also ensures that these would be well within the detector. Clearly, the loss in signal would be marginal as the final state there arises from decay of two scalar particles, with even the production cross-section not being strongly peaked. We also must ensure that the jets and the leptons are separated well enough to be detectable as individual entities. To this end, we adapt the well-known cone algorithm for jet separation to a parton-level analysis. Defining $\Delta R_{ab} \equiv \sqrt{(\Delta\eta_{ab})^2 + (\Delta\phi_{ab})^2}$ where $\Delta\eta$ is the difference of the rapidities of the two particles and $\Delta\phi$ is their azimuthal separation, we demand that

$$\Delta R_{jj} \geq 0.7 , \qquad \Delta R_{jl} > 0.5 , \qquad \Delta R_{ll} > 0.2 . \tag{7}$$

Detectability also requires that these particles (jets) must have a minimum momentum. Over and above this, it should be noted that the signal events would typically be characterized by all the four particles having relatively large transverse momenta (p_T). On the other hand, the SM background has a large component wherein at least one fermion pair has relatively small p_T. A cut on the particle momenta is thus called for. We find that rather than imposing the same requirement on all the particles, it is better to order them (leptons and jets individually) according to their p_T. However, in doing this, one must take into account the detector resolution effects. We incorporate this into our analysis by means of a rather conservative smearing of energies[5] [20]:

$$
\begin{aligned}
\frac{\delta E_j}{E_j} &= \frac{0.4}{\sqrt{E_j/1\ \mathrm{GeV}}} + 0.02 && \text{for jets ,} \\
\frac{\delta E_\ell}{E_\ell} &= \frac{0.15}{\sqrt{E_\ell/1\ \mathrm{GeV}}} + 0.01 && \text{for leptons .}
\end{aligned}
\tag{8}
$$

---

[5]The expected angular resolutions are too fine to be of any concern to us.

We then demand that

$$p_T^{j1}, p_T^{\ell 1} > 25 \,\text{GeV}, \quad p_T^{j2}, p_T^{\ell 2} > 20 \,\text{GeV}, \tag{9}$$

where $j1$ denotes the jet with larger transverse momentum *etc.*. Alongwith the separability requirement (eq.7), this also serves to eliminate the bulk of contributions from the $\gamma\gamma \to \ell^+\ell^-\gamma^*$ and $\gamma\gamma \to q\bar{q}\gamma^*$ diagrams.

As we have discussed before, the background also contains diagrams of the form $\gamma\gamma \to f\bar{f}Z^*$ with the Z going into the other pair of fermions. Eliminating these necessitates that we discard events where either the lepton-lepton or the jet-jet invariant mass is close to m_Z:

$$m_{\ell\ell}, m_{jj} \notin [80 \,\text{GeV}, 100 \,\text{GeV}]. \tag{10}$$

Imposing the above set of cuts, we can then calculate both the signal and background. For the latter, we need to sum over all possible light quarks[6]. Doing this, we obtain, for unpolarized beams and $\sqrt{s_{ee}} = 1 \,\text{TeV}$, an integrated cross-section of $\sigma_{\text{Bkgd}} = 2.32 \,\text{fb}$. To further improve the signal-to-noise ratio, we can use a particular feature of the signal event topology. In the limit of infinite momentum resolution, we can, for each of these events, find one particular lepton–jet pairing such that the corresponding invariant masses are exactly the same. Provided such a pairing is unambiguous, this invariant mass is then the mass of the squark. Clearly, the background events would not show the same characteristics, and this can be used to our advantage. We then retain only those events for which

$$\left| M_{\ell j}^{(1)} - M_{\ell j}^{(2)} \right| \leq 10 \,\text{GeV} \tag{11}$$

for at least one such pairing. The corresponding *average* mass is then treated as our determination of $m_{\tilde{q}}$. With this additional restriction, the background cross-section drops to $\sigma_{\text{Bkgd}} = 0.14 \,\text{fb}$. It might be argued, and rightly too, that a $m_{\tilde{q}}$ independent criterion as in eq.(11) is not the most efficient one. Indeed, with the fractional energy resolution growing with the jet/lepton energies, we would do better by optimizing this cut for each squark value that we might be interested in. However, we omit to do so in order to keep the analysis a simple one.

With the above set of kinematical cuts, we have been able to reduce the background to insignificant levels. It remains to be seen how much of the signal is retained and whether mass reconstruction is possible. We tackle the questions in the reverse order. The impediments to mass reconstruction come from two sources. The first is of course the effect of the resolution smearing. A second source of ambiguity is the possibility that both set of reconstructions could satisfy eq.(11). In such a case, we retain the pairing with the *larger* average (M_{av}) of the reconstructed masses. As is easily ascertained from Fig.3*a*, the mass reconstruction works quite well for relatively smaller values of $m_{\tilde{q}}$. For heavier squarks though, the peaks are not as sharp. This feature is easy to understand. As $m_{\tilde{q}}$ increases, the squarks are produced with smaller and smaller average momentum. Close to the kinematic threshold, the mass

---

[6]We do not consider here the special case that the squark decays into a lepton and b-quark thus making it possible for us to tag the corresponding jet.
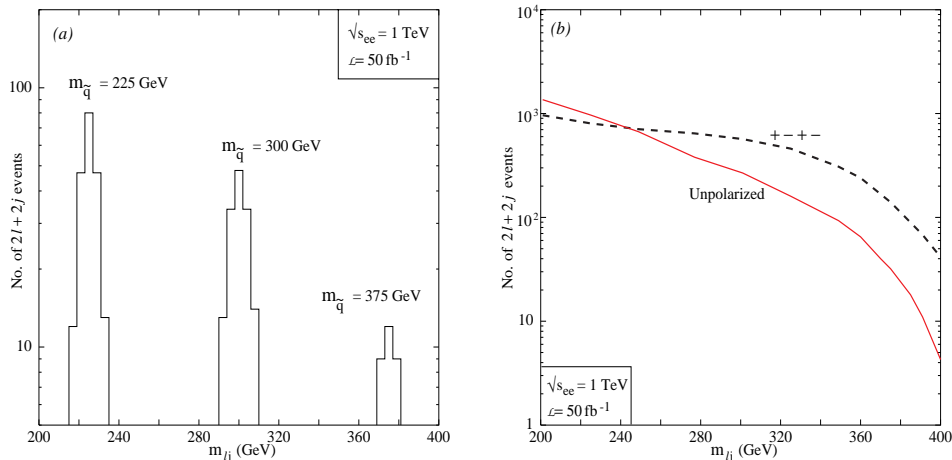
Figure 3: (a) *Mass reconstruction from the dilepton + dijet final mode at a photon-photon collider with the parent machine operating at center of mass energy of* $1\,\mathrm{TeV}$. *The cuts of eqs.(6–11) have been used. The SM background is much smaller than the scale of the graph.* (b) *Number of dilepton + dijet events due to squark production for both polarized and unpolarized initial beams.*

difference (eq.11), in the limit of infinite resolution, would vanish identically for *both* the pairings. Of course, if the resolution was really infinite, our algorithm—namely the larger of the two reconstructed masses—would still make the correct identification. However, because of the resolution smearing, migration of events do occur. Thus, sensitivity could be increased were we to compare, bin by bin, the data and the SM expectations, thereby using a statistical discriminator (such as a χ^2 test). In this article, though, we will not attempt such an analysis. Rather, we effect the somewhat cruder strategy of integrating over five contiguous bins[7] centering around M_{av} and ascribing any excess therein to a squark of mass M_{av}. The partial loss of information inherent in such a procedure makes our results to be somewhat conservative. In Fig.3*b*, we present the number of events expected (as a function of $m_{\tilde{q}}$) after the imposition of all of the above cuts (we assume here 100% branching into a lepton and a quark). Comparing it to Fig.1, we see that the loss in signal, while significant, is not debilitating. On the other hand, hardly any background events are expected within a given bin (the surviving background cross-section of 0.14 fb corresponds to just 7 events over the entire mass range for the assumed luminosity of $50\,\mathrm{fb}^{-1}$). Consequently, observation of even an handful of such events, concentrated within a small mass range, could be construed as the evidence for squark production and subsequent decay through an R-parity violating interaction, albeit with smaller branching fractions.

As we have commented in Section 3, in the supersymmetric case, the squark may

---

[7]As the lepton and quark momenta are smeared using a Gaussian distribution, the signal invariant mass distribution has not a sharp peak in the relevant mass bin. Rather it also shows a Gaussian structure. To take into account this smearing effect, when calculating the number of signal events for a particular squark or slepton mass, we not only consider the number of events in the relevant mass bin but also add to it the contribution from the four adjacent bins.

decay through R-conserving interactions into a quark and a chargino/neutralino. Although the latter will ultimately decay into SM particles through $\not{R}$ interactions, the event shape would be considerably different from that we have considered here. Confining ourselves solely to the analysis of 4-fermion final states, we can use the information of Fig.3b to obtain exclusion/discovery limits in the $m_{\tilde{q}}$–branching fraction plane. Since the number of background events is almost zero, the required branching fraction Br is approximately given by

$$\mathrm{Br} = \sqrt{\frac{n_{\mathrm{req}}}{N_s}}$$

where N_s is the number of signal events corresponding to $\mathrm{Br} = 1$ and $n_{\mathrm{req}} = 5\,(3)$ for discovery (95% exclusion). In Fig. 4 we present the corresponding contours for two different choices of the initial state polarisation. As the polarised $(+ - +-)$ cross-section dominates over the unpolarised for large $m_{\tilde{q}}$, the required branching ratios are consequently smaller. For example, close to the kinematic limit (say $m_{\tilde{q}} \approx 400$), we would make a discovery even with a branching fraction 50% provided we work with the correct beam polarisation. On the other hand, with an unpolarised initial state, and $m_{\tilde{q}} \gtrsim 390\,\mathrm{GeV}$, signal events number less than five even for a 100% branching.
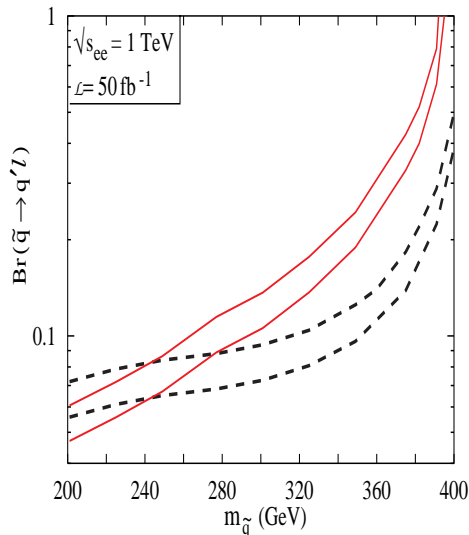

Figure 4: *Minimum branching ratio for the decay $\tilde{q} \rightarrow lj$ required for discovering (upper curve) or ruling out at 95% C.L. (lower curve) an up-type squark. The solid and dashed lines correspond to unpolarized and $(+ - +-)$ polarized initial states respectively.*

4.2 Slepton Production

The production cross-section for charged sleptons is higher (by a factor of $27/16$) than that for *up*-type squarks. However, since they decay into two quarks each, the

No	Subprocess type	Number of diagrams		Number of subprocesses
		$\mathcal{O}(\alpha\alpha_s)$	$\mathcal{O}(\alpha^2)$	
1.	$\gamma\gamma \to u_i \bar{u}_i gg$	30	0	2
2.	$\gamma\gamma \to d_i \bar{d}_i gg$	30	0	3
3.	$\gamma\gamma \to u_i \bar{u}_i u_i \bar{u}_i$	40	80	2
4.	$\gamma\gamma \to d_i \bar{d}_i d_i \bar{d}_i$	40	80	3
5.	$\gamma\gamma \to u\bar{u}c\bar{c}$	20	40	1
6.	$\gamma\gamma \to d_i \bar{d}_i d_j \bar{d}_j \ (i \neq j)$	20	40	3
7.	$\gamma\gamma \to u_i \bar{u}_i d_i \bar{d}_i$	20	71	2
8.	$\gamma\gamma \to u_i \bar{u}_i d_j \bar{d}_j \ (i \neq j)$	20	40	4
9.	$\gamma\gamma \to u\bar{c}d_i \bar{d}_j \ (i \neq j)$	0	31	3

Table 1: *Number of Feynman diagrams for various leading-order subprocesses contributing to $\gamma\gamma \to 4$ jets. i, j are the family indices.*

resultant final state of 4 jets is more complicated than that in the previous subsection. In Table. 1, we list the various subprocesses contributing to this background.

Despite the profusion of diagrams and the attendant complications, certain kinematical cuts suggest themselves. Drawing from the experience of the previous subsection, we demand that

$$|\eta_j| < 2.5 \ , \tag{12}$$

and

$$\Delta R_{jj} \geq 0.7 \ . \tag{13}$$

An important feature is that the background receives $\mathcal{O}(\alpha\alpha_s)$ contributions and that many more subprocesses contribute to it as compared to that in the previous subsection. Consequently, the background is much larger and we need to impose somewhat stricter p_T requirements. Once again ordering the jets by their transverse momentum, we demand that

$$p_T^{j1}, p_T^{j2} > 40 \,\mathrm{GeV}, \qquad \mathrm{p}_\mathrm{T}^{j3}, \mathrm{p}_\mathrm{T}^{j4} > 15 \,\mathrm{GeV} \ . \tag{14}$$

This helps us to eliminate the bulk of the $\mathcal{O}(\alpha\alpha_s)$ contributions. The $\mathcal{O}(\alpha^2)$ contributions, on the other hand, are dominated by the resonant contributions. In the present case, these are of two types : (i) $\gamma\gamma \to f\bar{f}Z^*$ as before, and (ii) $\gamma\gamma \to W^*W^*$. To eliminate both sets, we demand that

$$m_{ik} \notin [75 \,\mathrm{GeV}, 95 \,\mathrm{GeV}] \tag{15}$$

for any of the six pairings. Comparing it to the analogous cut of the last subsection, it might seem that a somewhat harder cut is called for. However, such a course would

entail the loss of a significant fraction of the signal as well. Unless we design $m_{\tilde{\ell}}$-specific cuts, eq.(15) was found to be an optimal choice. With these set of selection criteria, the processes of Table. 1 lead to a total of $\sigma_{\text{Bkgd}} \approx 170\,\text{fb}$ (for $\sqrt{s_{ee}} = 1\,\text{TeV}$).
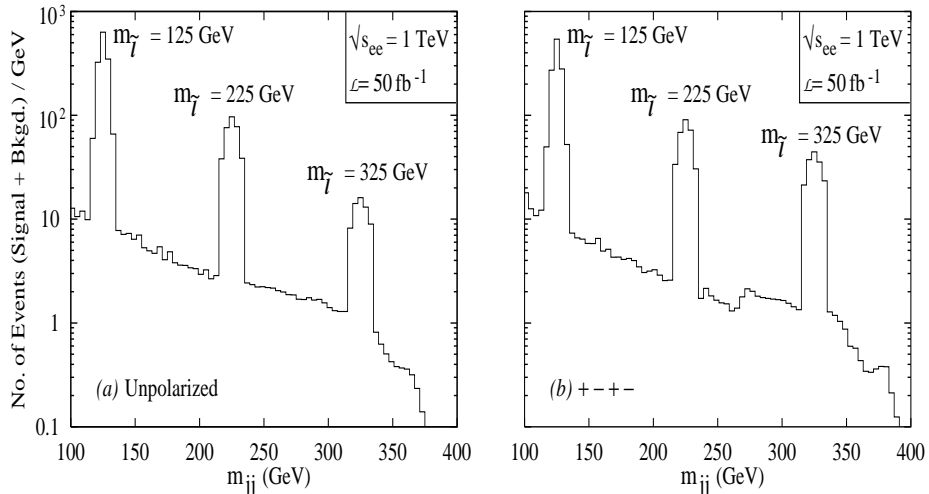

Figure 5: *Number of 4-jet events arising at a photon collider where the cuts of eqs.(12–16) have been imposed. The energy resolution is assumed to be the one given in eq.(8). Thge continuum corresponds to the SM background and the peaks to sleptons decaying into two quarks each.* (a) *is for unpolarised beams and* (b) *for polarised* $(+ - +-)$ *beams.*

As in the case of the squark, we again take recourse to mass reconstruction, demanding that

$$|M_{ij} - M_{kl}| \leq 10\,\text{GeV} \tag{16}$$

for at least one of the three pairings. Clearly, the combinatorial factor for the SM background is higher in this case than that for squark decays. Consequently, the reduction ($\sigma_{\text{Bkgd}} \rightarrow \approx 20$ fb) is not as pronounced. However, with most of this being concentrated at relatively small M_{av} (see Figs.5a,b), where the signal cross-section is on the higher side too, even this background is not a major source of concern. Also shown in Figs.5 are the signal profiles for particular values of $m_{\tilde{\ell}}$. The mass reconstruction is slightly worse here than that in the previous subsection. This is not unexpected as (i) jet energy resolution is significantly worse than lepton energy resolution; and (ii) here three different jet pairings are possible as compared to only two pairings in the other case. Still, there is a significant excess of signal events over the background. Since the latter is rather insensitive to beam polarization, a careful choice of the same can be used to further enhance this excess. An example of this is provided by Fig.5b.

To maximize sensitivity, we could either opt for mass-dependent kinematical cuts or compare events bin by bin and employ a statistical discriminator such as a χ^2 test. However, once again, we adopt the simpler course of summing over five contiguous bins centered around the slepton mass of interest and compare it with the background. Since the latter is no longer vanishingly small, we cannot simplify our analysis as in

the previous subsection. Instead, the required branching fraction is now given by

$$Br. = \sqrt{\frac{n\sqrt{N_b}}{N_s}}$$

where N_b and N_s are the number of background and signal events (summed over the 5 bins). $n = 5$ (2) for discovery (95 % C.L. exclusion). Of course, this algorithm is valid strictly in the large N_b limit; for small N_b, we use the appropriate Poisson limit. In Fig.6, we present the contours for two different polarization choices. For small sfermion masses, this channel is less sensitive compared to the one considered in the previous subsection, inspite of the larger production cross-section. This of course can be ascribed primarily to the much larger background and to a smaller extent to the combinatorial problem. For larger sfermion masses though, the background count is $\lesssim \mathcal{O}(1)$ for both cases. Hence the exclusion curves are quite similar in this region. Of course, with a larger integrated luminosity, this argument would cease to hold and the squark production channel would outperform the present one even for $m_{\tilde{f}}$ close to the kinematic limit.
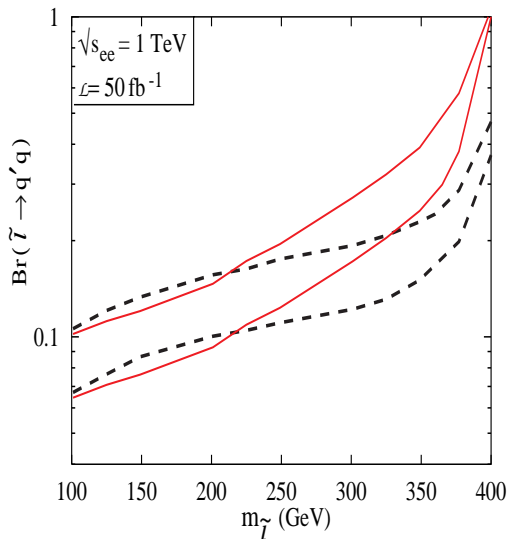

Figure 6: *Minimum branching ratio for the decay $\tilde{l} \rightarrow qq'$ required for discovering (upper curve) or ruling out at 95% C.L. (lower curve) a slepton. The solid and dashed lines correspond to unpolarized and $(+-+-)$ polarized initial states respectively.*

4.2.1   Sleptons decaying into b quarks

The above results can be significantly improved if the slepton were to decay into a b-quark and a light (u-type) quark. Since b-jets can be distinguished from those coming from light quarks or gluons, the number of processes contributing to the SM background is reduced considerably. Looking at Table 1, we see that, in the limit of

ideal identification [8], only one subprocess each of types (2 & 4) and two subprocesses each of types (6 & 8) may contribute. Consequently, the background, with the an identical set of cuts, is now reduced to $\lesssim 0.1$ fb.

This enormous reduction in the background more than offsets the reduction in the signal on account of the less-than-ideal b-tagging efficiency. For the latter, we use the conservative value $\epsilon_b = 0.6$ per b-jet [21]. An additional improvement occurs in the mass reconstruction on account of the smaller number of combinatorial possibilities. The situation is thus quite analogous to that of squark production, albeit with a smaller effective production cross-section (the ratio being $\sim 27\epsilon_b^2/16$). That the curves in Fig.7a are not exactly parallel to those of Fig.3b is due to the facts that the kinematic cuts are not exactly the same and that the energy resolution is slightly worse in the present case. The same also explains the shapes of the exclusion/discovery curves in Fig.7b.

Interestingly, despite the smaller backgrounds, b-tagging does not seem to help much for large slepton masses (compare the curves of Fig.6 and Fig.7b). This is easily understood on noticing the fact that the SM background is essentially zero for such invariant masses. Consequently, the sensitivity of the channel is determined by the signal size alone. With a less-than-ideal efficiency, b-tagging obviously reduces the signal size without gaining in terms of the background. Foregoing tagging would improve the efficiency (for large $m_{\tilde{l}}$) to the levels of Fig.6, but at the cost of determining the nature of the coupling.
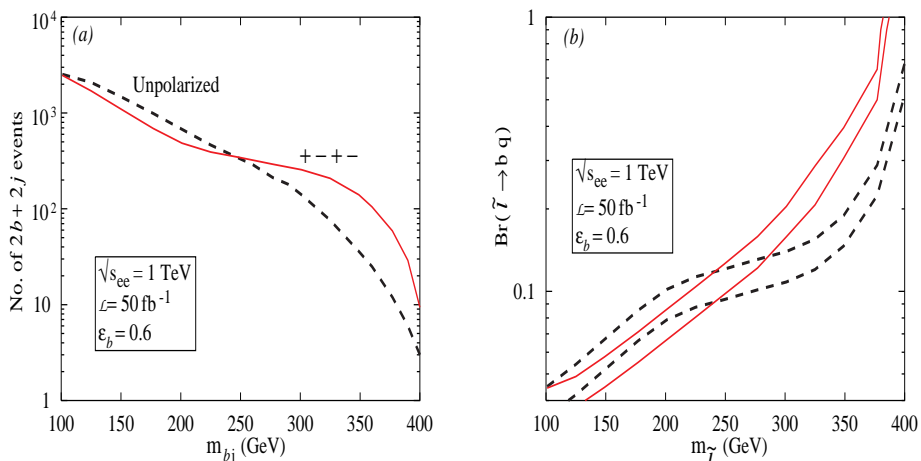

Figure 7: (a) *The number of* $2b$ - $2j$ *events coming from slepton production and decay; and* (b) *the minimum branching ratio for the decay* $\tilde{l} \to bq$ *required for discovering (upper curve) or ruling out at 95% C.L. (lower curve) a slepton. The solid and dashed lines correspond to unpolarized and* $(+ - +-)$ *polarized initial states respectively.*

---

[8]This approximation is quite valid given that misidentification probability $\lesssim 0.005$ even in a hadronic environment [21].

5 Bounds on the SUSY Parameter Space

In the previous sections we have presented the reach of a photon-photon collider in a *model independent* way. In other words, we have not made any assumptions about the decay modes allowed to these scalars. Once the rest of the spectrum in the theory (and their couplings with the scalar in question) is known, the branching fractions to a pair of SM fermions can then be computed in terms of the Yukawa coupling (as, for example, was done in section 3). The branching ratios can then be combined with the exclusion/discovery plots in a straightforward manner to yield the bounds on the relevant parameter space of the theory. For the sake of completeness, we present the outcome of one such exercise here.

As an illustrative example, we choose the case of a slepton decaying into a b and a light quark. The low energy bounds only imply

$$\lambda'_{113} < 0.021 \; \frac{m_{\tilde{f}}}{100 \text{ GeV}},$$

will all other relevant λ'_{ij3}s allowed to be larger. Thus we may, safely, choose $\lambda' = 0.02$ over the entire range of interest. In Fig.8, we present the discovery contours that are obtained by combining the results of our simulation (Fig. 7*b*) with the branching fractions of Fig. 2*a*.
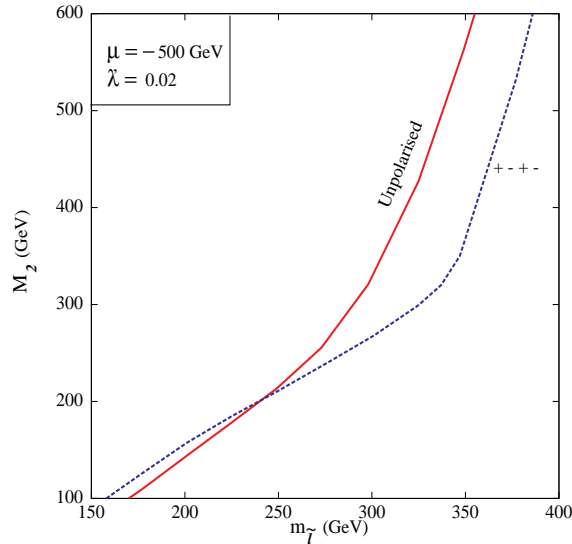

Figure 8: *Discovery contour in the M_2 - $m_{\tilde{l}}$ in the 2b- 2j channel for a (unpolarised) and b(polarised) case.*

The parameter space bounds as obtained from the other modes discussed in this paper are very similar. The case of the slepton decaying into two non-b quarks would, typically, lead to constraints slightly weaker than those of Fig.8. This is particularly true for smaller values of $m_{\tilde{l}}$. However, for slepton masses close to the kinematic limit, b-tagging actually reduces the sensitivity. Bounds derived from squark production, on the other hand, would depend crucially on the gluino mass. For small squark masses, decays into gluinos are unlikely and hence the bounds would be stronger than the ones

described by Fig.8. For large squark masses, on the other hand, the gluino channel might open up thus reducing the $\not R$ branching fraction drastically (see Figs.2) and thereby decreasing the efficacy of the search strategy discussed here.

Similar analyses obtain for leptoquarks and diquarks as well. In fact, the case of a generic diquark is almost exactly the same as that for the slepton, but for the modification in the cross section on account of a possibly differing electric charge. A generic leptoquark, on the other hand, provides for an additional two-body decay channel namely into a quark and a neutrino. While such a mode precludes mass reconstruction, it certainly can be used to improve the signal to noise ratio.

6   Conclusions

To summarise, we discuss scalar particle pair production at a photon photon collider and their subsequent 2-body decays through L violating interactions.

We find that the use of a few well-chosen kinematic cuts can eliminate the SM backgrounds to a considerable extent. Mass reconstruction is possible and is quite accurate almost over the entire kinematic range. For pair-production close to the threshold, the use of polarized electron and laser beams (used to obtain the high energy photons) can increase the production cross-sections manifold without significantly altering the SM background.

As the production cross-section is completely model-independent, the signal strength is a very good measure of the branching fractions into these L-violating decay modes. Consequently, bounds on the parameter space can be obtained, and we have done so for the case of R-parity violating supersymmetric models. Although slepton production cross sections are the largest, the corresponding backgrounds are larger too. This renders the discovery reach for this channel to be somewhat worse than that for up-type squarks decaying through a similar LQD coupling. However, if the slepton were to decay into a b-quark, then b-jet identification could be used to increase the sensitivity significantly and make it competitive with the up-squark channel.

It must be noted though that even if the L violating 2-body decay modes be small, the daughter particles from the L-conserving channels will finally decay through a L-violating mode. Such a cascading process will leave its own tell tale signature. An analysis, albeit a more complicated one, of the same would only serve to complement the present one. The discovery/exclusion plots presented here are thus only conservative ones and can be improved.

Finally, a study of B violating decays is but a straightforward extension of that presented in Section 4.2 of this article.

References

[1] J.C. Pati and A. Salam, Phys. Rev.**D10** (1974) 275.
   H. Georgi and S.L. Glashow, Phys. Rev. Lett. **32** (1974) 438;
   For reviews, see P. Langacker, Phys. Rep. **72** (1981) 185.

[2] H.P. Nilles, Phys. Rep. **110** (1989) 1;
H.E. Haber and G.L. Kane, Phys. Rep. **117** (1985) 75;
L. J. Hall and M. Suzuki, Nucl. Phys. **B231** (1984) 419;
S. Dawson, Nucl. Phys. **B261** (1985) 297;
S. Dimopoulos and L. Hall, Phys. Lett. **B207** (1987) 210.

[3] See, for example, J.L. Hewett and T.G. Rizzo, Phys. Rep. **183** (1989) 193 and references therein.

[4] See, for example, W. Buchmüller and D. Wyler, Phys. Lett. **B177** (1986) 377;
W. Buchmüller, R. Rückl and D. Wyler, Phys. Lett. **B191** (1987) 442; Erratum: *ibid.***B448** (1999) 320;
also see S. Davidson, D. Bailey and B. Campbell Z. Phys. C**61** (1994) 613.

[5] P. Fayet, Phys. Lett. **B69** (1977) 489;
G. Farrar and P. Fayet, Phys. Lett. **B76** (1978) 575.

[6] D. Choudhury and S. Raychaudhuri, Phys. Lett. **B401** (1997) 54;
G. Altarelli *et al.*, Nucl. Phys. **B506** (1997) 3;
H. Dreiner and P. Morawitz, Nucl. Phys. **B503** (1997) 55;
J. Kalinowski *et al.*, Z. Phys. C**74** (1997) 595;
T. Kon and T. Kobayashi, Phys. Lett. **B409** (1997) 265;
G. Altarelli, G.F. Giudice, and M.L. Mangano, Nucl. Phys. **B506** (1997) 29;
J. Ellis, S. Lola, and K. Sridhar, Phys. Lett. **B408** (1997) 252;
M. Carena, D. Choudhury, S. Raychaudhuri and C.E.M. Wagner, Phys. Lett. **B414** (1997) 92.

[7] B. Armbruster *et al.*(KARMEN collab.), Phys. Lett. **B348** (1995) 19;
B. Zeitnitz, talk given at NEUTRINO'98, Takayama (1998);
R. Maschuw, talk given at WIN'99, Cape Town (1999);
D. Choudhury and S. Sarkar, Phys. Lett. **B401** (1996) 87;
D. Choudhury, H. Dreiner, P. Richardson and S. Sarkar, Phys. Rev.**D61** (2000) 095009.

[8] Y. Fukuda *et al.* (Super-Kamiokande collab.), Phys. Rev. Lett. **81** (1998) 1562;
Phys. Lett. **B436** (1998) 33.

[9] B. Abbott *et al.*(D0 Collab.), hep-ex/9907019, Phys. Rev. Lett. **83** (1999) 4476.

[10] F. Abe *et al.*(CDF Collab.), Phys. Rev. Lett. **83** (1999) 2133;
D. Choudhury and S. Raychaudhuri, Phys. Rev.**D56** (1997) 1778.

[11] C. Adloff *et al.*(H1 Collab). Eur.Phys.J. **C11** (1999) 447.

[12] Stringent limits on products of *R*-parity violating couplings are given by K. Agashe and M. Graesser, Phys. Rev.**D54** (1995) 4445;
F. Vissani and A.Yu. Smirnov, Phys. Lett. **B380** (1996) 317;
D. Choudhury and P. Roy, Phys. Lett. **B378** (1996) 153.

[13] S. Chakrabarti, D. Choudhury, R. Godbole and B. Mukhopadhyaya, Phys. Lett. **B434** (1998) 347.

[14] I.F. Ginzburg *et al.*, *Nucl. Inst. Meth.* **205** (1983) 47; *ibid.* **219** (1984);
V. Telnov, Nucl. Inst. Meth., **A 355**(1995) 3.

[15] G. Bhattacharyya, Nucl. Phys. B (Proc. Suppl.) **52A** (1997) 83;
H. Dreiner, (electronic archive: hep–ph/9707435 v2);
R. Barbier *et al.*, (electronic archive: hep–ph/9810232);
J.L. Goity and M. Sher, Phys. Lett. **B346** (1995) 69; erratum: *ibid.* **385** (1996) 500;
B.C. Allanach, A. Dedes and H. Dreiner, Phys. Rev.**D60** (1999) 075014.

[16] V. Barger, G.F. Giudice, and T. Han, Phys. Rev.**D40** (1989) 2987;
G. Bhattacharyya and D. Choudhury, Mod. Phys. Lett. **A10** (1995) 1699.

[17] Some recent studies are, M. Drees, S. Pakvasa, X. Tata and T. ter Veldhuis, Phys. Rev.**D57** (1998) 5335; E.J. Chun and J.S. Lee, hep-ph/9811201; A. Abada and M. Losada, hep-ph/9908352; S. Rakshit, G. Bhattacharyya and A. Raychaudhuri, Phys. Rev.**D59** (1999) 091701.

[18] H. Klapdor-Kleingrothaus *et al.*, Prog. Part. Nucl. Phys. **32** (1994) 261; J. W. F. Valle, (electronic archive: hep–ph/9509306); K.S. Babu and R.N. Mohapatra, Phys. Rev. Lett. **75** (1995) 2276; G. Bhattacharyya, H. Klapdor-Kleingrothaus and H. Pas, Phys. Lett. **B463** (1999) 77.

[19] W.F. Long and T. Stelzer, Comp. Phys. Comm. **81**, (1994) 357.

[20] H. Murayama and M. Peskin, Ann. Rev. Nucl. Part. Sci. **46** (1996) 533.

[21] D. Amidei and C. Brock, "Report of the TeV2000 Study Group on Future EW Physics at Tevatron", 1995.